

Upper Jurassic-Lower Cretaceous Source-Rock Evaluation and Oil—Source Rock Correlation in the Abadan Plain, Southwest Iran

Mehdi Kobraei^{a, *}, AhmadReza Rabbani^{a, **}, and Farid Taati^b

^aAmirkabir University of Technology, Faculty of Petroleum Engineering, Tehran, Iran

^bNIOC, Khazar Exploration and Production Company, Geology Department, Tehran, Iran

*e-mail: mehdi.kobraei@gmail.com

**e-mail: rabbani@aut.ac.ir

Received September 17, 2018; revised December 28, 2018; accepted January 17, 2019

Abstract—Eight oil samples from Lower Cretaceous Fahliyan reservoirs and 51 core and cutting samples from Upper Jurassic-Lower Cretaceous Garau Formation in Abadan Plain, Southern Iran, were analyzed using bulk property and molecular methods in order to identify their geochemical characteristics such as maturity and source depositional environment, as well as to correlate them to respective source rock(s). Rock-Eval pyrolysis and vitrinite reflectance measurements indicated that the Garau Formation, classified as a good-to-excellent source rock, the kerogen is mainly of Type II and the maturity is in peak oil generation. The crude oils of the Fahliyan reservoir are classified as light oil (API more than 35), non-biodegraded, saturate fraction, slight even/odd predominance, and front-end biased distribution in gas chromatogram. According to molecular and isotopic data, the oils were generated by a marine carbonate source rock which was deposited under the anoxic condition. Furthermore, all the studied samples reveal compositional similarity and hence can be assigned to one oil family, originating from a common source rock. Based on compositional similarities of biomarkers and isotope data in the studied crude oils and source rock, the Upper Jurassic-Lower Cretaceous Garau Formation can be regarded as the main source rock of the oils.

Keywords: Cretaceous, Fahliyan Formation, Crude Oil, Abadan Plain, oil-source correlation

DOI: 10.1134/S0016702919070073

1. INTRODUCTION

The Abadan Plain basin in Southwestern Iran comprises more than 7 oil producing fields which are producing from a reservoir in the Cretaceous age (Fig. 1). Cretaceous reservoirs such as the Khami and Bangestan groups are the main oil producers in the Zagros basin containing oil in this region (Motiei, 2010). In addition, the existence of gas condensate has been proved in the Jurassic succession. Although the Abadan Plain is regarded as one of the most important hydrocarbon regions in the Iran, its petroleum system has been poorly studied geochemically.

The most important source intervals in the Abadan Plain include Middle Jurassic Sargelu Formation and Upper Jurassic-Lower Cretaceous Garau Formation which were investigated in an initial study (Kobraei et al., 2019(1, 2)) and are presented in other publications (Zeinalzadeh and Sajjadian, 2009; Abeed et al., 2011).

The Abadan Plain is located in the Southeastern part of the Mesopotamian basin in Iraq. Using a geochemical study and 3D basin modeling, Pitman et al. (2004) showed that all the oils in the Jurassic-to-Cre-

taceous reservoir are generated by a Middle Jurassic source interval. However, Abeed et al. (2012) later pointed out that hydrocarbon in the Cretaceous interval is produced from the Upper Jurassic-Lower Cretaceous Sulaiy Formation (time equivalent of Garau Formation in the Abadan Plain). It is believed that oils from Lower Cretaceous-to-Eocene age can be divided in two groups based on maturity parameters.

The present study which is the complementary part of an initial study on geochemical investigation of the Lower Cretaceous petroleum system (Kobraei et al., 2017) presents a detailed description of oils discovered in the Fahliyan (Lower Cretaceous) reservoir in the region. The first step was to characterize geochemical parameters in the Cretaceous oils. Then, the biomarker composition in the studied samples was classified and finally, using oil-oil and oil-source correlation, the oil family and respective source rocks were identified.

2. GEOLOGICAL SETTING

The Abadan Plain area is situated within the fore-land basin Southwest of Zagros Mountain. There is no outcrop evidence from underlying structures (Fig. 1).

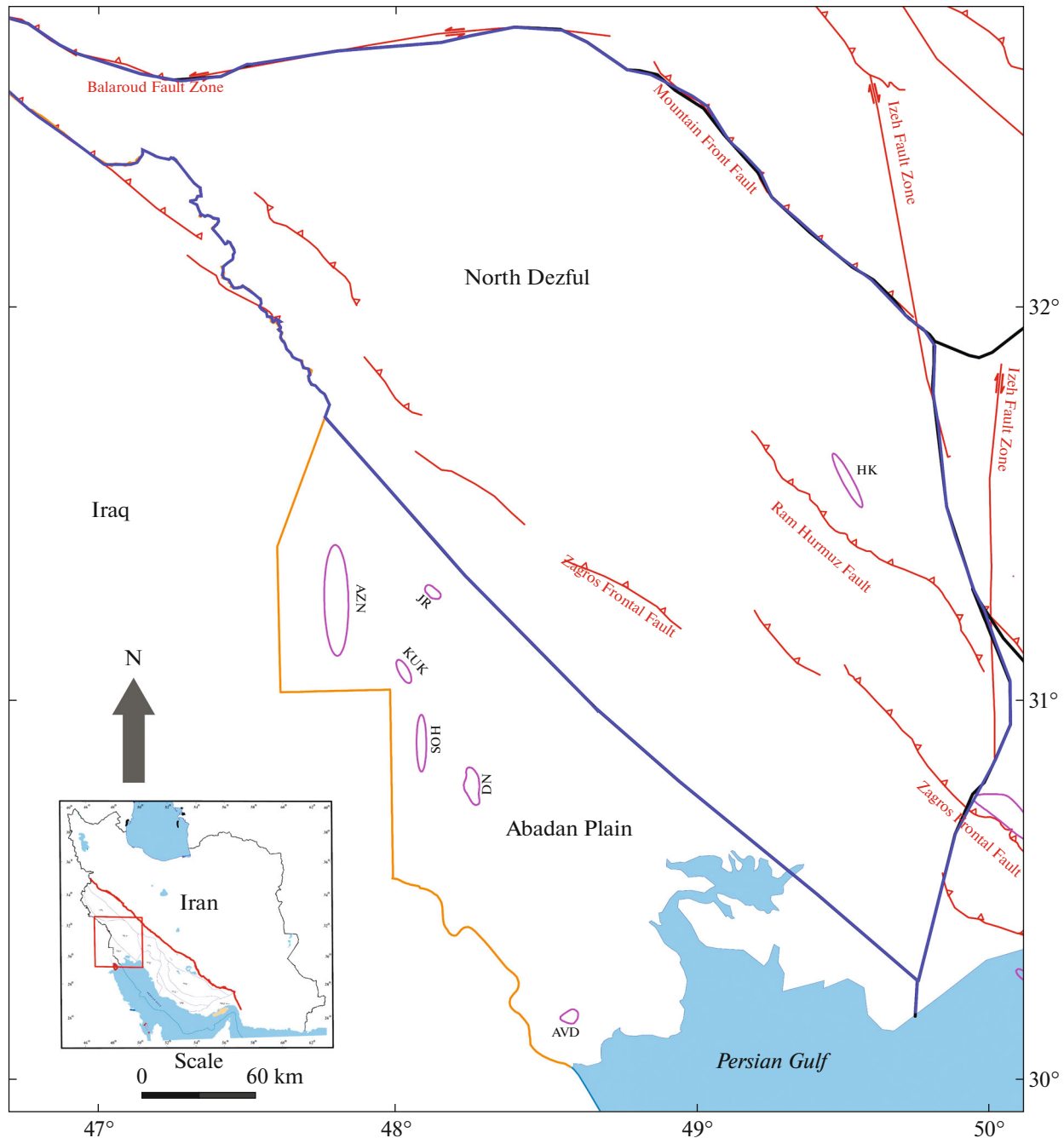


Fig. 1. Map of the studied area and oil fields in the Abadan plain basin with main tectonic boundaries (Adapted from Zeinalzadeh et al., 2015).

The Zagros fold and thrust belt have been formed from Late Miocene to the present due to continent-continent collision between the Arabian and the Eurasian plates (Stocklin, 1974).

Results of seismic interpretation and integrated analysis of well data shows three main deformations in the area: (1) NW–SE-oriented Middle-Upper Cretaceous compression, (2) NE–SW-oriented compression associated with the generation of the Zagros fold and thrust

belt, and (3) N–S-oriented structures which are located along the elongate, narrow anticline. This N–S structures originated during the Late Proterozoic Natibah orogeny and were reactivated during the Permo-Carboniferous, Mesozoic, and Tertiary, possibly related to the movement of Infracambrian salt (Satarzadeh et al., 2000; Jassim and Goff, 2006; Aqrabi et al., 2010).

Abadan Plain did not tolerate the active tectonic movement which put it in a passive margin setting

with no significant erosion events (AbdollahieFard et al., 2006). In addition, little erosion was reported in the Mesopotamian basin in Southern Iraq (Abeed et al., 2013).

Prolific Jurassic-to-Cretaceous source rocks, long burial history, good reservoir/seal pairs, and a generally late migration history have played major roles in the configuration of traps and charging events in the Abadan Plain area.

This study focuses on the geochemical investigation of crude oils from Fahliyan (Lower Cretaceous) Formation which is one of the most prolific reservoirs, and Garau Formation as the most important source interval in the studied area (Fig. 2).

The Garau Formation consists of five units in the Abadan plain area. The bottom unit consists of dark grey to black carbonaceous shale and dark argillaceous pyritic limestone (James and Wynd, 1965). Overlying this, is dark grey limestone with carbonaceous shale. Above this, is grey to brown shale, and above that, is limestone with black nodules. The upper part of the formation is alternating grey shale with shaley limestone, and glauconitic sandy limestone and sandy marls in the uppermost part. Almost all of the Garau Formation is considered to have been deposited under a low-energy anoxic environment, and it has excellent source rock potential, especially in the lower part (Fig. 2).

The Lower Cretaceous Fahliyan Formation is dominated by carbonate lithology which is often dolomitized. It is deposited in a shallow-water carbonate ramp which has been formed due to the uplifting of Abadan Plain area (Sharland, 2001).

3. MATERIALS AND METHOD

A total of 51 core and cutting samples representing the Garau Formation as the main Lower Cretaceous source rock from six exploration wells drilled in the Southwestern part of the Zagros basin were chosen for geochemical analyses. In addition, 8 oil samples from Lower Cretaceous Fahliyan reservoir were obtained from 8 wells in three different oil fields in the studied region. The oil and rock samples were subjected to elementary and complementary geochemical analyses, explained in the following sections.

3.1. Rock-Eval Pyrolysis and Vitrinite Reflectance

The most widely used method to identify the generation potential of source rocks is Rock-Eval pyrolysis (Espitalié et al., 1977). In the present study, rock samples from source intervals were pyrolyzed using a Rock-Eval 6 instrument with a module to identify the total organic carbon (TOC) content, free hydrocarbon fraction (S1), the fraction released by thermal cracking (S2), and the pyrolysis temperature (T_{max}) of maximum kerogen cracking at the top of the S2 peak, as described by Espitalié et al. (1977). Some additional

geochemical parameters such as production potential (S1 + S2), HI (S2/TOC), OI (S3/TOC), and PI (S1/S1 + S2) were also calculated and are listed in Table 1. For more details about pyrolysis and interpretation, refer to Tissot and Welte (1984).

For Rock-Eval pyrolysis, 7 samples were selected for measuring vitrinite reflectance. Measurements were taken out using Zeiss Axipolan II microscope in oil immersion; following the method described by Taylor et al. (1998). The results can be seen in Table 1.

3.2. Complementary Analysis

In this study, oil samples from 8 wells aligned with 4 rock extract samples from source intervals were subjected to preliminary geochemical experiments such as API, asphaltene precipitation, and column chromatography, to be fractionated to saturate, aromatic, and resin, using 5 mL *n*-pentane (Fraction 1), 5 mL *n*-pentane/DCM (40/60 v/v, Fraction 2), and 5 mL MeOH/DCM (50/50 v/v, Fraction 3). Then, complementary stages such as gas chromatography (GC), gas chromatography-mass spectrometry (GC-MS), and stable isotope analysis were performed on the selected samples.

GC analysis was performed by a gas chromatograph equipped with a 30 m DB-1 fused silica capillary column (i.d. 0.25 mm; 0.25 μ m film thickness). For the mass spectrometry analysis, the GC was coupled with a Finnigan MAT GCQ ion trap mass spectrometer. The oven temperature was set from 70 to 300°C at the rate of 4°C/min, in which 15 min was considered as the isothermal period. The injection temperature was 275°C in the split-less mod, and the carrier gas was helium.

The results were processed with a Finnigan data system. Relative percentages and absolute concentrations of different saturate and aromatic compound families were calculated based on comparison of peak areas from the gas chromatograms and those of published internal standards (Moldowan et al., 1985; Radke et al., 1990; Weiss et al., 2000).

The isotopic composition ($\delta^{13}C$) of oils and source rock extracts in saturate and aromatic fractions were analyzed utilizing combustion in the presence of oxygen at 1020°C using an elemental analyzer (Flash EA 1112). The generated CO₂ was measured directly in a Thermo-Fisher SELTA V isotope ratio mass spectrometer. The precision of the total procedure was in the range of $\pm 0.1\%$.

In order to analyze carbon isotope ratio for each individual alkane, the GC-ultra was attached to a Delta V isotope-ratio mass spectrometer (IRMS) via a combustion interface (GC IsoLink) and an auto-dilution unit (ConFlow IV). The gas column specification which had been coupled was the same as the one described above, and the temperature program was the same as the one for conventional GC-MS analysis. Carbon isotope ratios for individual alkanes were calcu-

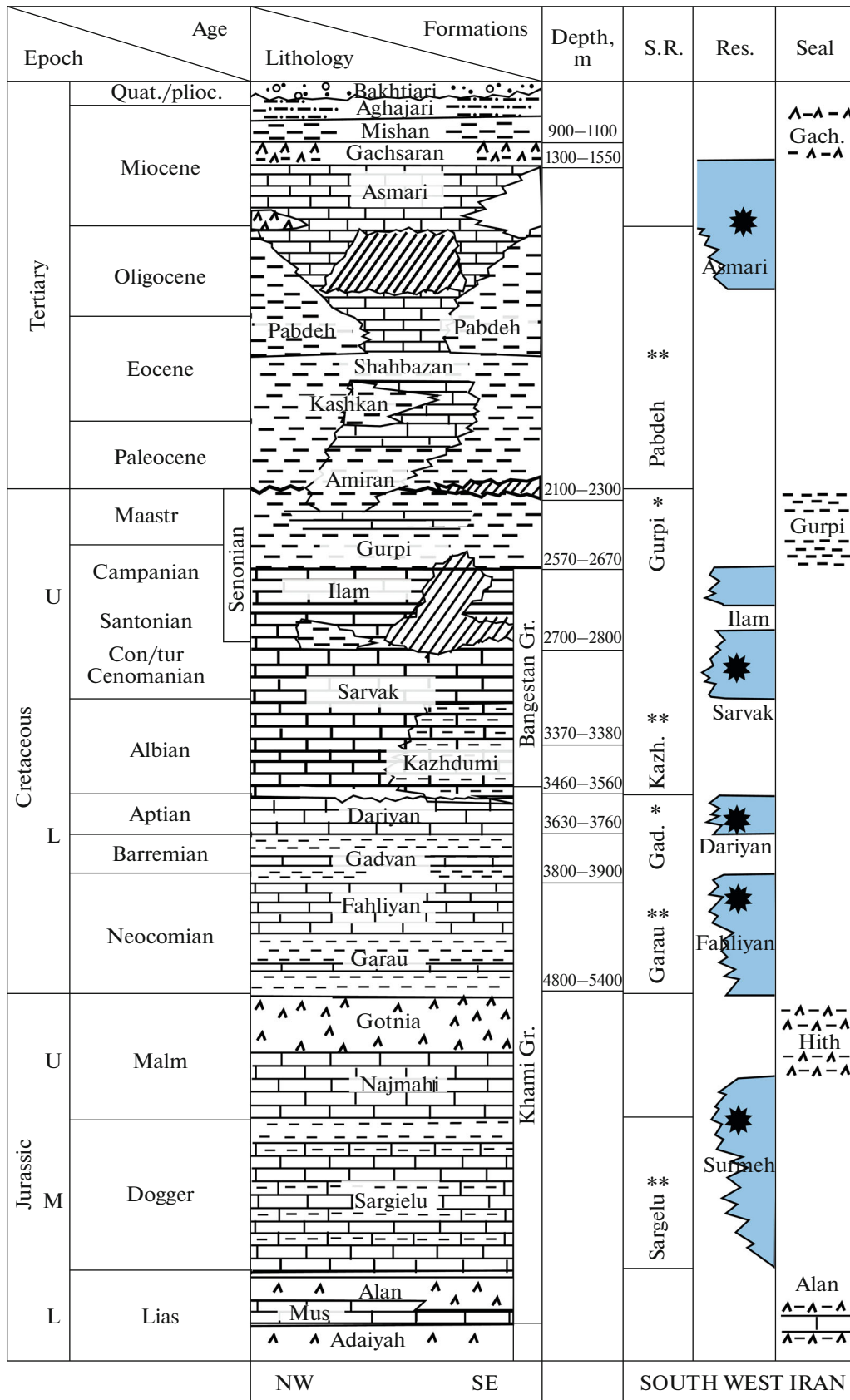


Fig. 2. Stratigraphic chart of the studied area in Southwest Iran (Adapted from Bordenave and Hegre, 2010).

Table 1. Rock-Eval pyrolysis data for the Garau Formation in the studied wells, South West Iran

Oil Field	Formation/ ID	Dept, m	TOC, wt %	SI ₁ , mg HC/g Rock)	S ₂ , mg HC/g Rock)	S ₃ , mg HC/g Rock)	T _{max} , °C	HI, mg HC/g Rock)	OI	PI	VRo
DN	Garau-1	4650	1.1	1.07	2.58	0.47	438	234	43	0.29	—
DN	Garau-2	4656	1.25	2.18	4.22	0.64	438	337	51	0.34	—
DN	Garau-3	4700	2.1	1.7	2.99	0.61	439	142	29	0.36	1.01
DN	Garau-4	4750	1.87	1.22	3.15	0.77	440	168	41	0.28	0.82
DN	Garau-5	4765	0.86	3.21	1.72	0.59	441	200	69	0.65	—
DN	Garau-6	4830	1.52	1.92	4.21	0.79	440	277	52	0.31	0.84
DN	Garau-7	4880	1.82	2.22	3.93	0.71	439	217	39	0.36	0.88
DN	Garau-8	4905	2.22	2.18	5.85	0.62	440	263	28	0.27	—
DN	Garau-9	4950	0.58	0.63	0.94	0.41	438	162	70	0.4	—
DN	Garau-10	4970	0.62	0.1	2.25	0.72	442	360	116	0.04	—
JR	Garau-11	4670	0.69	1.13	0.84	1.92	434	122	278	0.57	—
JR	Garau-12	4860	1.52	4.08	4.64	0.76	442	305	50	0.47	—
JR	Garau-13	4895	1.11	4.58	3.68	0.73	444	331	66	0.55	—
JR	Garau-14	4920	0.76	3	2.18	0.72	443	287	95	0.58	—
JR	Garau-15	4935	0.42	1.21	1.16	0.58	441	276	139	0.51	—
JR	Garau-16	4980	0.43	1.18	1.08	0.39	443	253	92	0.52	—
JR	Garau-17	4990	0.66	2.18	1.5	0.83	442	227	126	0.59	—
JR	Garau-18	5015	0.64	2.44	2.05	0.5	443	321	78	0.54	—
JR	Garau-19	5105	2.46	9.15	6.69	1.61	445	272	66	0.58	0.93
JR	Garau-20	5120	2.56	7.24	8.22	1.69	453	321	66	0.47	—
JR	Garau-21	5200	4.16	9.85	8.53	1.55	449	205	37	0.54	—
JR	Garau-22	5345	1.91	6.97	5.62	2.32	445	294	121	0.55	—
JR	Garau-23	5360	1.78	8.11	4.49	2.25	437	252	126	0.64	—
JR	Garau-24	5375	1.2	5.1	3.83	1.48	442	320	124	0.57	—
JR	Garau-25	4664	1.26	0.91	2.86	0.73	434	227	58	0.24	—
JR	Garau-26	4714	3.17	5.03	4.71	1.03	434	149	32	0.52	—

Table 1. (Contd.)

Oil Field	Formation/ ID	Dept, m	TOC, wt %	S1, mg HC/g Rock)	S2, mg HC/g Rock)	S3, mg HC/g Rock)	T _{max} , °C	HI, mg HC/g Rock)	OI	PI	VRo
JR	Garau-27	4706	3.24	1.15	8.23	1.88	443	254	58	0.12	—
JR	Garau-28	4756	2.98	2.4	5.09	1.17	433	171	39	0.32	—
JR	Garau-29	4776	2.48	1.07	5.55	1.17	442	224	47	0.16	—
JR	Garau-30	4666	2.4	0.8	9.33	1.24	442	389	52	0.08	—
JR	Garau-31	4906	3.85	7.98	8.95	1.63	440	232	42	0.47	—
HK	Garau-32	3300	1	1.2	1.47	0.25	440	147	25	0.45	—
HK	Garau-33	3450	0.98	0.82	0.99	0.44	441	101	45	0.45	—
HK	Garau-34	3580	1.15	0.77	1.25	0.82	443	108	71	0.38	—
HK	Garau-35	3600	1.97	1.2	2.42	1.04	444	123	53	0.33	—
HK	Garau-36	3700	2.75	1.11	1.89	1.16	444	68	42	0.37	—
HK	Garau-37	3800	1.42	0.87	1.25	0.88	445	88	62	0.41	—
HK	Garau-38	4050	2.22	0.43	0.97	0.95	446	43	43	0.31	—
HK	Garau-39	4150	1.1	0.65	1.71	0.62	448	155	56	0.28	—
HK	Garau-40	4250	1.25	0.88	1.92	0.95	447	153	76	0.31	—
YAD	Garau-41	4550	6.42	14.4	5.33	0.51	438	83	8	0.73	—
YAD	Garau-42	4624	6.02	6.09	3.11	0.48	438	52	8	0.66	—
YAD	Garau-43	4655	3.88	1.86	2.74	0.31	442	71	8	0.40	—
YAD	Garau-44	4695	5.72	1.22	3.85	1.43	441	67	25	0.24	—
YAD	Garau-45	4810	3.56	2.85	3.92	0.53	442	110	15	0.42	—
YAD	Garau-46	4850	10.8	10.7	13.05	0.54	442	121	5	0.45	1.01
YAD	Garau-47	5100	2.3	1.05	3.7	0.69	443	161	30	0.22	—
YAD	Garau-48	4502	0.92	4.74	3.77	0.35	440	410	38	0.56	—
YAD	Garau-49	5116	4.21	1.15	3.27	0.51	441	77	12	0.26	—
YAD	Garau-50	5152	1.53	4.81	3.99	0.60	442	261	39	0.55	—
YAD	Garau-51	5170	1.48	5.65	4.01	0.55	445	271	37	0.58	0.88

Abbreviations: HI: Hydrogen Index (S2/TOC); OI: Oxygen Index (S3/TOC); PI: Potential Index (S1/ (S1 + S2)).

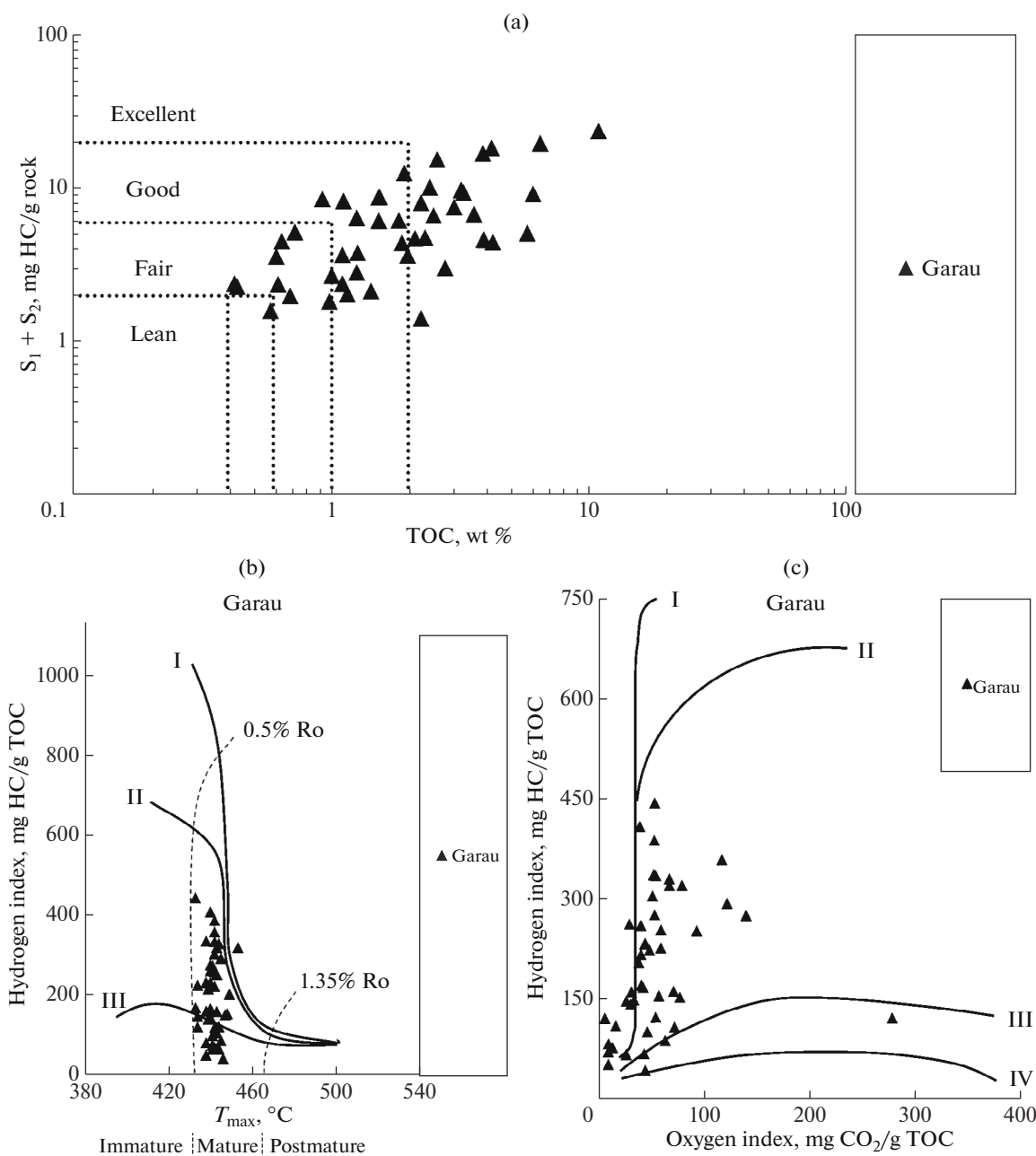


Fig. 3. (a) Plot of $S_1 + S_2$ versus TOC showing the production potential of the studied samples (Peters and Cassa, 1994). (b and c) HI versus T_{max} (left) and OI (right) showing the maturity and kerogen type of the studied samples (Hunt, 1996).

lated using CO₂ as a reference gas that was automatically introduced in to the IRMS at the beginning and the end of each analysis. The data were reported in ‰ relative to the Vienna Pee Dee Belemnite standard. Repeated analyses showed high precision, and the standard deviation of each compound was less than $\pm 0.5\%$.

4. RESULTS

4.1. Source Rock Geochemistry

The present total organic carbon content of Garau Formation varies from 0.42 to more than 10 wt %, and

the average TOC in this Formation is about 2.2 wt % (Table 1) which can be classified as a good-to-very good potential source rock (Hunt, 1996). In the analyzed samples, S_2 changes between 0.84 and 13 mg HC/g Rock which places the Garau Formation in the very good source rock groups. According to the plot of $S_1 + S_2$ (production potential) versus TOC in Fig. 3a, the present production potential in the Garau Formation can be considered as fair to very good (Peter and Cassa, 1994).

HI is plotted versus T_{max} and Oxygen Index in the plots of Figs. 3b, 3c in order to identify the kerogen type

Table 2. Result of Bulk oil composition, API gravity and GC analysis for saturated hydrocarbon fraction of crude oils from the Fahliyan reservoir, Abadan plain

Sample ID	Sat. %	Aro. %	Pol. %	API	Pr/ nC_{17}	Ph/ nC_{18}	Pr/Ph	CPI	$nC_{17}/(nC_{17} + nC_{27})$	$nC_{18}/(nC_{18} + nC_{19})$	TAR
Fh-AZN	86.16	7.21	6.64	37	0.20	0.37	0.66	1.01	0.94	0.56	0.40
Fh-KUK	33.71	33.71	32.57	38	0.46	0.50	0.65	0.96	0.56	0.47	0.94
Fh-HOS	53.19	23.64	23.17	33	0.39	0.45	0.79	0.96	0.59	0.51	0.82
Fh-HOS	55.6	27.02	17.38	36	0.36	0.50	0.78	1.11	0.76	0.53	0.55
Fh-KUK	54.5	21	24.5	38.5	0.28	0.6	0.52	1.07	0.91	0.58	0.41
Fh-HOS	54	27.5	18.5	36.5	0.23	0.52	0.51	0.98	0.81	0.55	0.51
Fh-AVD	63	28	9	42	0.18	0.31	0.68	0.99	0.82	0.52	0.08
Fh-JR	57	30	13	38	0.39	0.49	0.9	1.02	0.74	0.52	0.27
Garau-6	57.5	15.5	27	—	0.7	0.8	0.41	1.01	0.9	0.6	0.35
Garau-30	61	12	27	—	0.49	0.62	0.5	1.06	0.96	0.61	0.14
Garau-37	52	16	32	—	0.31	0.68	0.68	1.01	0.89	0.63	0.35
Garau-45	46.5	16.5	37	—	0.4	0.63	0.8	1.08	0.91	0.68	0.15

Abbreviation: Sat = saturates; Aro = aromatics; Res = resins; Asp = Asphaltenes; API = API gravity; Pr/Ph = pristane/phytane; CPI = $2(nC_{23} + nC_{25} + nC_{27} + nC_{29})/[nC_{22} + 2(nC_{24} + nC_{26} + nC_{28}) + nC_{30}]$; TAR = $(nC_{27} + nC_{29} + nC_{31})/(nC_{15} + nC_{17} + nC_{19})$.

and maturity of organic matter in the Garau Formation. As shown in the graphs, kerogen is of Type II which is in consistence with paleogeographic maps of depositional time of Garau Formation and kerogen type II-S for Sulaiy Formation in the Mesopotamian basin in Iraq (Abeed et al., 2011; Kobraei et al., 2017-2).

The maturity of Garau Formation was determined on the basis of T_{max} , PI, and vitrinite reflectance. In the studied rock samples, T_{max} values change from 433 to 453°C with an average of 442°C. Vitrinite reflectance has been measured for 7 samples which yield around 0.9% (Table 1). According to the plot of HI versus T_{max} in Fig. 3b, as well as vitrinite reflectance measurement, the maturity of organic matter in the Garau Formation can be identified as peak oil generation.

It is noteworthy that the Garau samples are already close to the peak of oil expulsion window. Therefore, initial values of both S2 and HI of Garau samples could have been much higher, even double the current values. Then the Garau Formation could be classified as very good to excellent source rock.

4.2. Oil Geochemistry

Oil characterizations. The results of API measurement and liquid chromatography for composition detection in the oil samples are shown in Table 2. The oils show API gravity between 33 to 42 which classifies them in the light oil group. Most of oils show a dominance of saturate fraction which ranges from 33 to more than 80%.

Regarding GC data, the Fahliyan reservoir oils are characterized by slight even/odd predominance, higher concentration of short chain alkanes (front

end-biased distribution), high values of nC_{17}/nC_{27} , CPI values near unity, and Pr/Ph ratio less than one (Table 2 and Fig. 4a).

High values of API as well as existence of short-chain normal alkanes ($<n-C_{15}$), no UCM in the GC chromatograms and very low concentration of C_{28} BNH (17α 25 Nor-Hopanes) in the saturates GC-MS fragmentograms shows no biodegradation in the studied oils (Peters et al., 2005).

4.2.1. Oil maturity. The very low ratios of Pr/ nC_{17} and Ph/ nC_{18} which are plotted in Figure 5 shows an advanced level of maturity (Hunt, 1996), no biodegradation (Volkman, 1998), and reducing depositional environment of source rock (Hunt, 1996).

In the C_{29} steranes (5α (H), 14α (H), 17α (H)), as maturity increases, the isomerization at C-20 will increase the 20S/ (20S + 20R) ratio from 0 to 0.5 (Peters et al., 2005). Here, this ratio ranges from 0.47 to 0.55 (Table 3) which approves a high level of maturity in the studied oil samples. Peter et al. (2005) showed that due to the increase in maturity, the isomerization in the C-14 and C-17 in the C_{29} regular steranes increases the amount of $\beta\beta/(\beta\beta + \alpha\alpha)$ ratio from 0 to 0.7 (equilibrium at 0.67–0.71). In the Fahliyan oil samples, this ratio is in the range of 0.54 to 0.61 (Table 3).

With increasing the maturity of organic, C_{27} 17α -tris-norhopane (Tm) is less stable than C_{27} 18α -tris-norneohopane (Ts). Ts/(Ts + Tm) ratio is sensitive to lithology of source rock, for example, oils from carbonate source rocks have lower ratios compared to shale generated oils (Peters et al., 2005). Ts/(Ts + Tm) has been considered for further investigation of maturity in the studied oil samples. According to the Ts/(Ts + Tm) ratios which range from 0.4 to 0.7 (Aver-

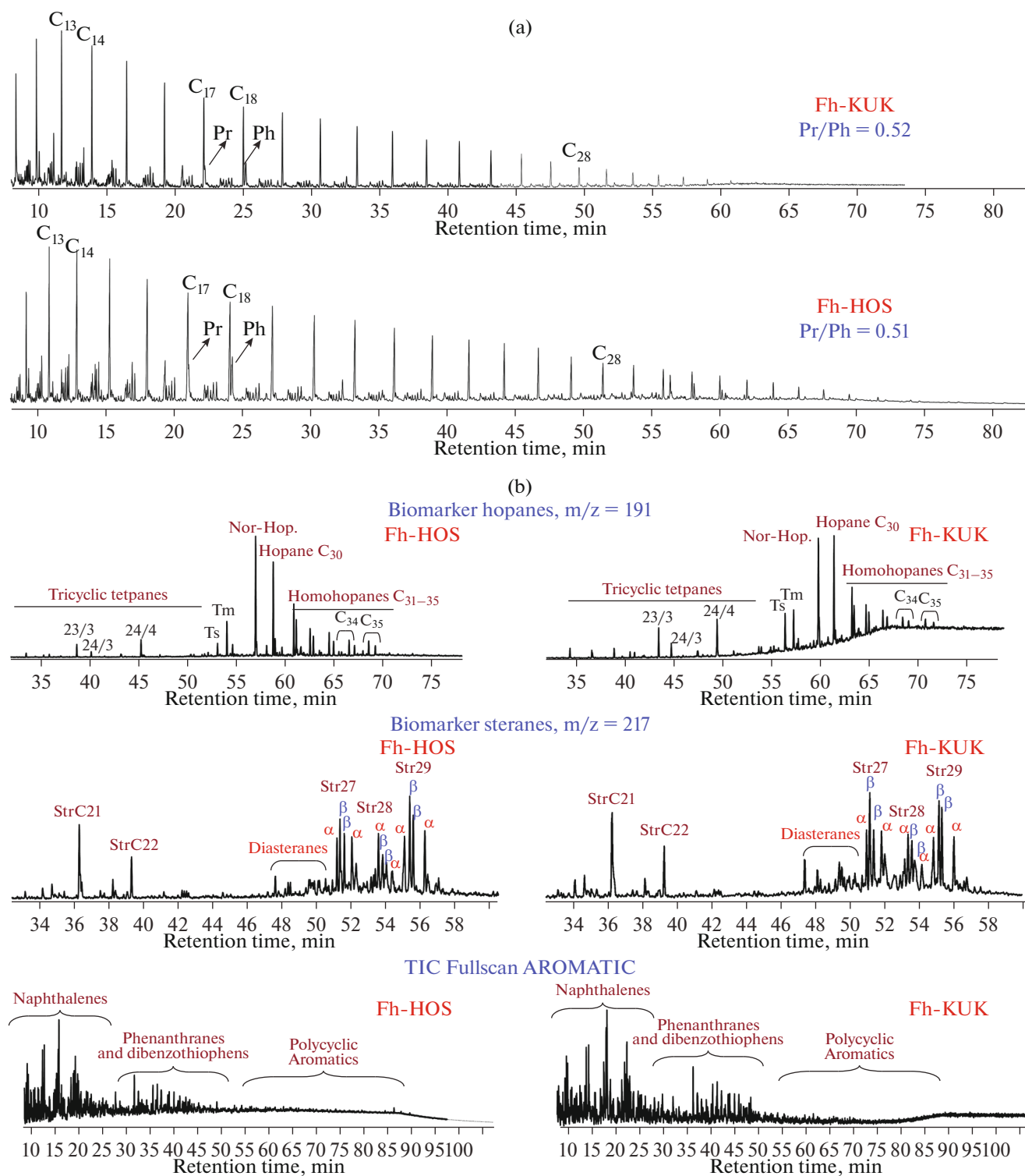


Fig. 4. (a) GC-SAT chromatograms for 2 selected oil sample in the Fahliyan reservoir. (b) Typical saturate and aromatic GC-MS fragmentograms of 2 selected Fahliyan oil samples.

age 0.57) in the Table 3, the Fahliyan reservoir oil samples can be regarded in the advanced level of maturity.

In the aromatic compound with increasing maturity, the value of 4-MDBT/1-MDBT (methyl diben-

zothiophene) ratio will increase in the oil and rock extract. In the studied samples, this value is more than 2 which shows advanced level of maturity in the oil and rock samples.

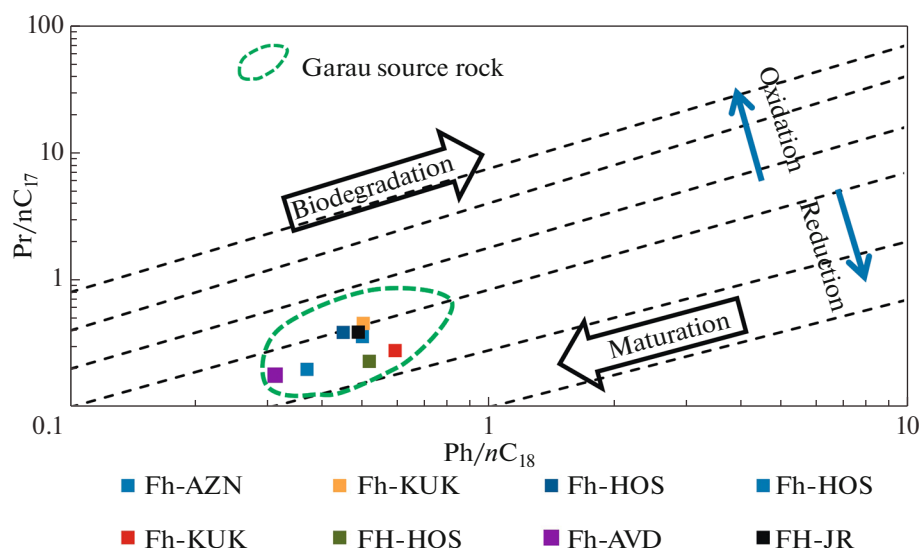


Fig. 5. Plot of $\text{Pr}/n\text{C}_{17}$ versus $\text{Ph}/n\text{C}_{18}$ from GC-FID showing maturation, depositional environment, and kerogen type in the studied source and oil samples (After Hunt, 1996).

4.2.2. Source depositional environment of oils. Very low $\text{Pr}/n\text{C}_{17}$ and $\text{Ph}/n\text{C}_{18}$ ratios (Fig. 5), prevalence of short-chain alkanes, Pr/Ph ratio less than 1, TAR less than 1, and front end-biased distribution in gas chromatograms (Fig. 4a) show marine algae and deposition under the marine anoxic condition in the source rock (Peters et al., 2005; Tissot and Welte, 1984).

Peters et al., (2005) believed that in regular steranes, C_{27} sterane contributes to marine organic matter, while C_{29} shows input of terrestrial organic matter into the depositional environment. In the studied samples, the ternary diagram of relative distribution of regular steranes shows low amount of C_{29} -steranes, indicating a limited contribution of higher plants. Based on Fig. 6, there is a shift toward C_{27} , indicating the marine carbonate source rock.

Very low gammacerane index (abundance of gammacerane versus C_{30} hopane) indicates there is no high salinity and water stratification in the source depositional environment (Zhang et al., 1988; Table 3).

The low concentrations of C_{19} and C_{20} tricyclic terpanes are typical for marine carbonate composition source rock (Aquino Neto et al., 1983). The lower concentration of overall tricyclic terpanes as well as higher concentration of C_{23} tricyclic terpanes may indicate marine depositional environment. Furthermore, the lower values of $\text{C}_{26}/\text{C}_{25}$ (less than 0.9) as well as high ratio of $\text{C}_{29}/\text{C}_{30}$ hopane (more than 0.6) and $\text{C}_{34}\text{S}/\text{C}_{35}\text{S}$ homohopanes (more than 0.8) show a prevalent marine carbonate depositional environment (Subroto et al., 1991; Peters et al., 2005; Table 3).

In aromatic biomarkers, the dibenzothiophene/phenanthrene (DBT/P) ratio is plotted versus Pr/Ph (Fig. 7a) which indicates marine carbonate as a

source environment for the studied oil samples (Hughes, 1995).

Furthermore, according to the mentioned geochemical parameters, all the studied samples reveal compositional similarity and, hence, can be assigned to one oil family, originating from a common source rock.

Bulk composition stable carbon isotope analysis has been applied to show the depositional environment of studied oil samples (Table 4). Moreover, individual n -alkanes GC-IRMS were measured (Fig. 7c) for further oil-oil and oil-source correlation, shown in Figs. 7b, 7c. Figure 7b shows the plot of $\delta^{13}\text{C}$ aromatic versus saturates (Sofer, Z., 1984), according to which all the oil samples are located in a marine environment.

Using statistical processing on the isotope analysis results, a parameter known as Canonical Variable (CV) can be calculated (Sofer, Z., 1984). Regarding Table 4, the CV index confirms the results, because for all oil samples the CV is less than 0 which means the reduction of marine depositional environment.

The average $\delta^{13}\text{C}$ values of n -alkanes (C_{15} – C_{29}) for the studied oils ranges from -29 to -29.3‰ . Small changes (lower than 2‰) indicate that all the studied samples are derived from the same source (Clayton, 1991; Peters et al., 2005; Galimov, 2006; Alizadeh et al., 2016).

Figure 7c shows n -alkane isotope profiles for 2 oil samples in the Fahliyan Formation and 2 rock samples from Garau Formation as the most important source rock in the Upper Jurassic and Lower Cretaceous succession. There is an acceptable similarity in isotope profiles of all the studied oil and rock samples.

Table 3. Saturate and Aromatic biomarker ratios of crude oils and from Fahliyan reservoir and the Garau source rock extracts, Abadan Plain

Sample ID	%C ₂₇ (217)	%C ₂₈ (217)	%C ₂₉ (217)	Str29 ββ/(ββ + αα)	Str29 20S/(20S + 20R)	DBT/Phen	23/3 Tri/24/4 Tetra	C ₂₆ /C ₂₅ Tri	Ts/(Ts + Tm)	C ₂₉ /C ₃₀ Hopane	C ₃₅ /C ₃₄ S HomHopane	4- MDBT/1- MDBT
Fh-AZN	46	20	34	0.61	0.50	1.50	2.20	0.80	0.61	1.20	0.85	—
Fh-KUK	39	23	39	0.57	0.54	1.10	1.11	0.76	0.42	0.94	0.92	2.25
Fh-HOS	34	25	41	0.55	0.52	1.36	0.67	0.80	0.48	1.25	0.60	3.12
Fh-HOS	34	24	43	0.54	0.55	1.02	0.63	0.73	0.46	1.33	0.65	2.85
Fh-KUK	33	28	39	0.58	0.54	1.20	2.19	0.75	0.51	1.34	0.98	2.76
Fh-HOS	32	20	48	0.54	0.52	1.25	2.73	0.50	0.40	1.27	1.04	2.56
Fh-AVD	53	18	29	0.56	0.54	2.82	3.72	0.43	0.74	1.42	0.90	4.0
Fh-JR	28	28	44	0.56	0.47	1.36	0.87	0.80	0.58	1.02	1.00	3.31
Garau-6	39	28	33	0.63	0.48	1.91	—	—	0.67	1.1	0.84	3.2
Garau-30	45	26	29	0.51	0.5	1.77	—	—	0.45	1.3	0.83	1.0
Garau-37	30	33	37	0.48	0.38	3.44	—	—	0.70	1.16	0.90	2.15
Garau-45	44	26	29	0.53	0.42	3.25	—	—	0.41	0.95	0.86	2.8

Abbreviation: %C₂₇ = %C₂₇ steranes/(%C₂₇-%C₂₉ steranes); %C₂₈ = %C₂₈ steranes/(%C₂₇-%C₂₉ steranes); %C₂₉ = %C₂₉ steranes/(%C₂₇-%C₂₉ steranes); DBT/P = Dibenzothio-phenes/Phenanthrene; 23/3 Tri/24/4 Tetra = 23 ticyclic terpanes/24 tetracyclic terpanes; C₂₆/C₂₅ Tri = C₂₆/C₂₅ tricyclic terpanes; Ts/(Ts + Tm) = 18a(H)-trisnorhopane/[18a(H)-trisnorhopane + 17a(H)-trisnorhopane]; MDBT = Methyl Dibenzothiophene.

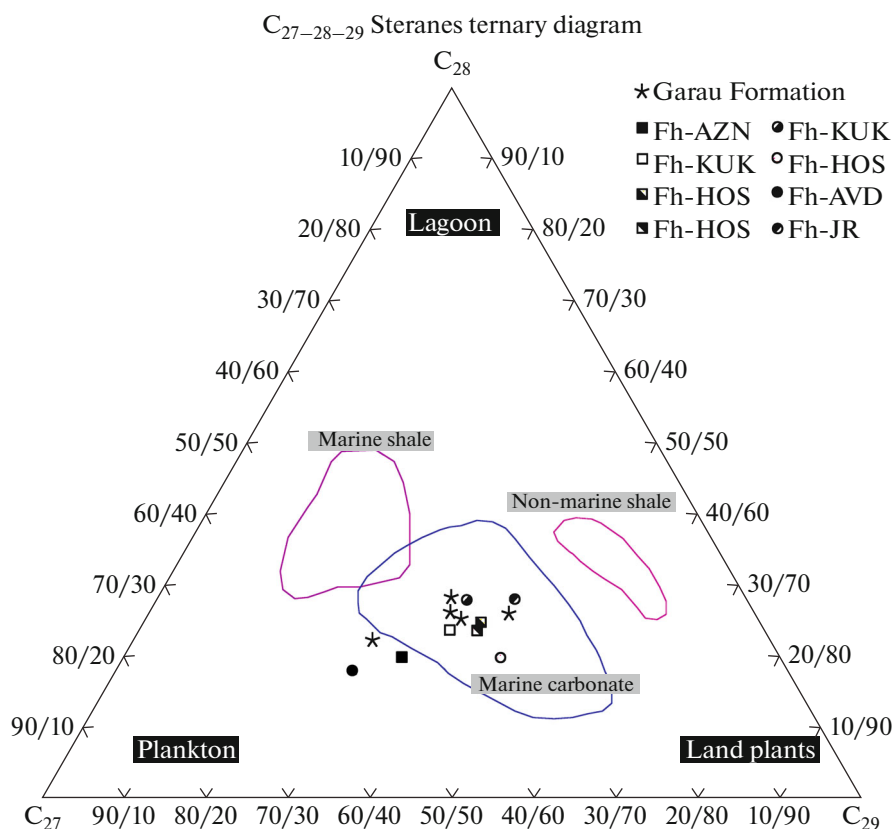


Fig. 6. Ternary diagram of C_{27} – C_{28} – C_{29} steranes for the studied oil and rock samples (After Peters et al., 2005).

4.3. Oil-Oil and Oil-Source Correlation

According to the compositional analysis (Table 2), crude oils from the Fahliyan Formation in the Abadan Plain can be classified as paraffinic oils (Tissot and Welte, 1984). Figure 5 plots Pr/nC_{17} vs. Ph/nC_{18} showing a narrow cluster which means very good similarity in all the studied oil samples. Moreover, there is good correlation between Garau source rock and the oil samples.

The highest-quality source rocks in the study area are the Upper Jurassic-Lower Cretaceous marine carbonates Garau Formation (time equivalent in Iraq is the Sulaiy Formation) and Middle Jurassic Sargelu Formation (Pitman et al., 2004; Abeed et al., 2011; Kobraei et al., 2017(1)).

In the previous section, it was mentioned that the higher amount of C_{27} regular steranes relates to higher contribution of marine organic matter. The triangle diagram in Figure 6 reveals a remarkable similarity among the oil samples themselves and between the oil and Garau source rock samples.

The marine carbonate source rock is further proved as the origin of Fahliyan reservoir oils by the relationship between Pr/Ph and the dibenzothiophene/phenanthrene (DBT/Ph) in Fig. 7a. The source rock was deposited in a marine carbonate

environment, as also shown by the relationship in Fig. 7b.

Based on normal alkane isotope profiles, almost all the studied oils are derived from a common source (Fig. 7c). The profile in this figure shows a very high correlation between oils and rock samples from Garau Formation. Here, the more negative $\delta^{13}C$ values indicate a higher contribution of planktonic algae (Herzcg and Fairbanks, 1987; Murray et al., 1994).

Table 4. Result of bulk isotope analysis in the studied samples

Sample ID	Saturated HC	Aromatic HC	CV ^a
	$\delta^{13}C$ (PDB)	$\delta^{13}C$ (PDB)	
Fh-AZN	–27.5	–26.4	–1.9881
Fh-HOS	–27.1	–25.8	–1.6076
Fh-HOS	–27.0	–25.6	–1.4773
Fh-AVD	–26.9	–26.5	–3.8161
Garau-30	–29.2	–28.0	0.3
Garau-37	–29.0	–27.9	–0.1
Garau-45	–27.2	–26.1	–0.6

^a CV = $(-2.53 \delta^{13}C_{Sat} + 2.27 \delta^{13}C_{Aro}) - 11.65$ (Sofer, 1984).

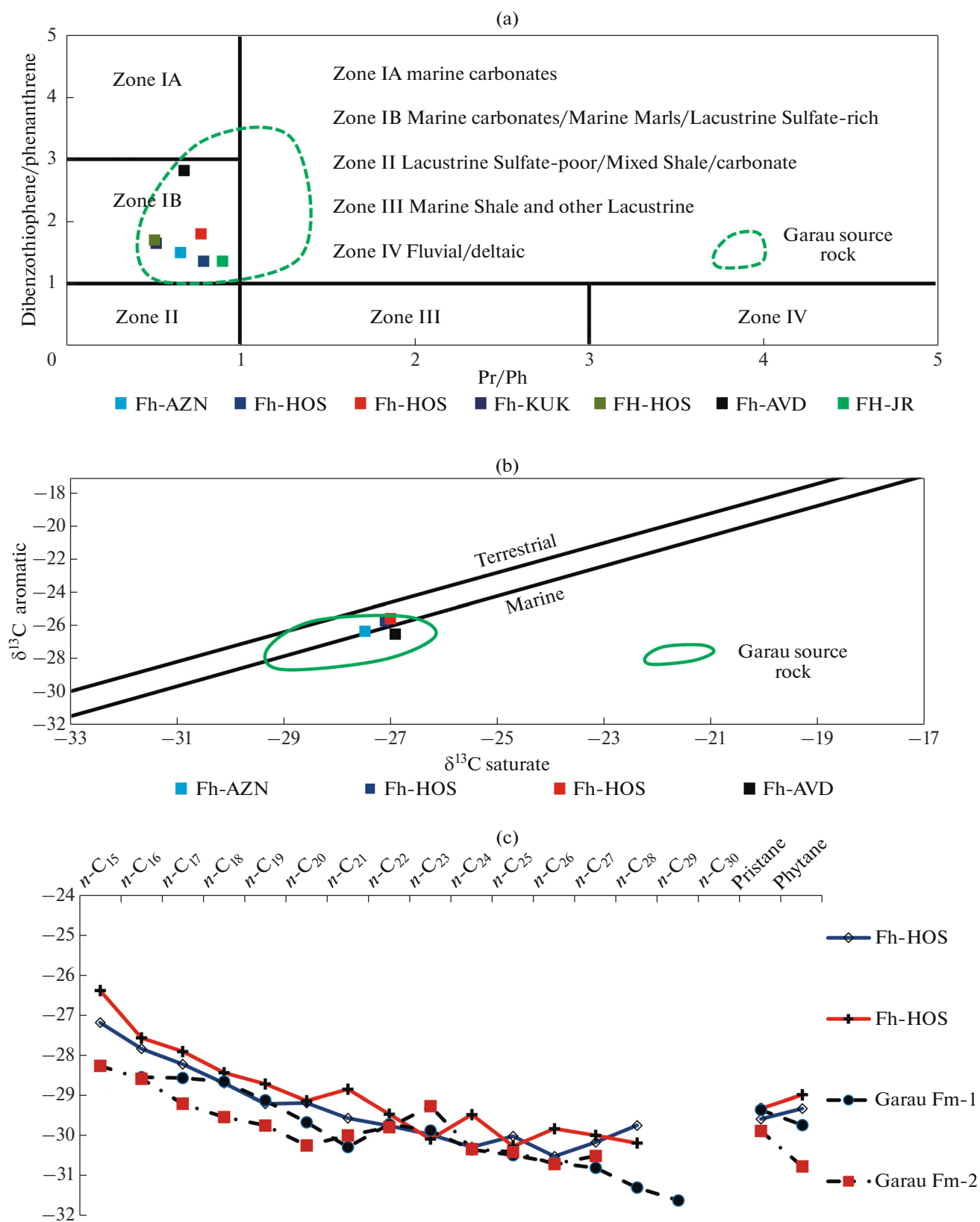


Fig. 7. (a) Plot of DBT/P versus Pr/Ph for the oil and rock samples (Hughes et al., 1995). (b) Plot of $\delta^{13}\text{C}$ aromatic versus saturate to investigate the organic matter depositional environment (Sofer, 1984). (c) Plot of n -alkanes GC-IRMS profile for 4 rock and oil samples.

Alizadeh et al. (2016) found that Cretaceous reservoir oils (including Gurpi, Ilam, Sarvak, Kazhdumi, Gadvan, and Fahliyan formations) are derived from Kerogen Type IIS of a marine carbonate lithology. Moreover, other studies of oil-source rock correlation for equivalent source/reservoir rock successions in Iraq and Kuwait indicate that the Sulaiy Formation (time equivalent of Garau Formation) appears to be the potential source rock candidate based on molecular and bulk isotope geochemistry (Abdullah and Connan, 2002; Abeed et al., 2012). Sargelu Formation is another source rock interval in Middle Jurassic succession in Southwestern Iran which can be regarded as the origin of Fahliyan reservoir oils. Pitman et al. (2004) believed that most of the oils in the Cretaceous petroleum system of Iraq are generated by Jurassic Sargelu Formation. The main problem for Jurassic source suggestion is the presence of Gotnia Formation with more than 200 m of thickness and evaporite in lithology which cover the area as a blanket. It is very difficult to propose migration for any hydrocarbon across such an ideal seal, although some faults can be seen in seismic lines which start from deeper Jurassic intervals, move up through the Gotnia Formation, and finally die out in the Garau Formation (Kobraei, 2016). These faults could act as conduits for the migration of generated Jurassic hydrocarbon into the overlying strata.

5. CONCLUSION

Results of Rock-Eval analysis indicated that the Upper Jurassic-Lower Cretaceous Garau Formation, with an average TOC of 2.1 wt % and HI value of 213 mgHC/g TOC, can be classified as a good-to-excellent source rock. The production potential of the Garau Formation improves both to the East and West of the study area. The kerogen type in the Garau Formation is mainly Type II. According to T_{max} values, the plot of HI versus T_{max} and vitrinite reflectance measurement, the maturity of organic matter in Garau Formation can be regarded as peak oil generation.

The crude oils of the Lower Cretaceous Fahliyan reservoir in the Abadan Plain area are classified as light oil (API values of more than 35). They showed dominance of saturate fraction, slight even/odd predominance, and front end-biased distribution in the GC profile.

Maturity indication parameters such as Pr/nC_{17} , Ph/nC_{18} , Hopane, steranes, and aromatic biomarker ratios show an advanced level of maturity in the studied oil. Furthermore, some other studies in the area showed that oils in the Lower Cretaceous reservoirs are generated in the late maturity stage of source rocks (Abeed et al., 2012; Alizadeh et al., 2016).

The oils are derived from kerogen Type II of marine carbonate source rocks, further indicated by very low Pr/nC_{17} and Ph/nC_{18} ratios, Pr/Ph and TAR ratios of

less than 1, regular sterane distribution, very low gammacerane and oleanane indices, low concentration of tricyclic terpanes, and DBT/P ratio of more than 1.

Stable carbon isotope analysis results (including bulk and individual n-alkanes) for the studied oils reveals marine depositional environment of source rock and no diversity between their organic matter inputs.

Based on similar biomarker and isotope correlation parameters, the most likely source rock of the studied oils is Upper Jurassic-Lower Cretaceous Garau Formation. The Garau Formation which is in the peak oil generation started to generate and expel hydrocarbon from late Cretaceous.

6. ACKNOWLEDGMENTS

The authors would like to thank the National Iranian Oil Company Exploration Directorate for providing samples, data, and financial support of geochemical analysis. We are also grateful to the Geochemistry Department of NIOCEXP and Department of Geology for helpful discussions and comments which improved the original manuscript.

REFERENCES

- I. Abdollahi-Fard, A. Braathen, M. Mokhtari, and A. Alavi, "Interaction of the Zagros fold-thrust belt and Arabian-type, deep-seated folds in the Abadan plain and the Dezful embayment, SW Iran," *Petrol. Geosci.* **12** (4), 347–362 (2006).
- F. H. Abdullah and J. Connan, "Geochemical study of some Cretaceous rocks from Kuwait: comparison with oils from Cretaceous and Jurassic reservoirs," *Org. Geochem.* **33**, 125–148 (2002).
- Q. Abeed, A. Alkhafaji, and R. Littke, "Source rock potential of the upper Jurassic-Lower Cretaceous succession in the southern Mesopotamian basin, Southern Iraq," *J. Petrol. Geol.* **34** (2), 117–134 (2011).
- Q. Abeed, D. Leythaeuser, and R. Littke, "Geochemistry, origin and correlation of crude oils in Lower Cretaceous sedimentary sequences of the southern Mesopotamian Basin, southern Iraq," *Org. Geochem.* **46**, 113–126 (2012).
- Q. Abeed, R. Littke, F. Strozyk, and A. K. Uffmann, "The upper Jurassic-Cretaceous petroleum system of southern Iraq: a 3-D basin modeling study," *GeoArabia* **18**, 179–200 (2013).
- B. Alizadeh, H. Saadati, M. Rashidi, and M. Kobraei, "Geochemical investigation of oils from Cretaceous to Eocene sedimentary sequences of the Abadan Plain, Southwest Iran," *Mar. Petrol. Geol.*, **73**, 609–619 (2016).
- A. A. M. Aqrabi, J. C. Goff, A. D. Horbury, and F. N. Sadooni, "The petroleum geology of Iraq". (Scientific Press, Beaconsfield, 2010).
- F. R. Aquino Neto, J. M. Trendel, A. Restle, J. Connan, and P. A. Albercht, "Occurrence and formation of tricyclic and tetracyclic terpanes in sediments and petroleum," *Organic Geochemistry*, Ed. by M. Bjoroy, P. Albrecht, and C. Cornfold (John Wiley & Sons, New York, 1981), pp. 659–676 (1983).

- M. L. Bordenave and J. A. Hegre, "Current distribution of oil and gas fields in the Zagros Fold Belt of Iran and contiguous offshore as a result of the petroleum systems," *Geol. Soc. London, Spec. Publ.* **330**, 291–313 (2010).
- C. J. Clayton, "Carbon isotope fractionation during natural gas generation from kerogen". *Mar. Petrol. Geol.* **8**, 232–240 (1991).
- J. Espitalié, J. L. Laporte, M. Madec, F. Marquis, P. Lepat, and J. Paulet, "Méthoderapide de caractérisation des roches mères, de leur potentiel pétrolier et de leur degré d'évolution," *Rev. l'Institut Français du Pétrole* **32**, 23–45 (1977).
- Galimov, E.M. "Isotope organic geochemistry," *Org. Geochem.* **37**, 1200–1262 (2006).
- A. L. Herczeg and R. G. Fairbanks, "Anomalous carbon isotope fractionation between atmospheric CO₂ and dissolved inorganic carbon induced by intense photosynthesis," *Geochim. Cosmochim. Acta* **52**, 895–899 (1987).
- J. M. Hunt, *Petroleum Geochemistry and Geology*, 2nd ed., (W.H. Freeman and Company, New York, 1996).
- W. B. Hughes, A. G. Holba, and L. I. P. Dzou, "The ratios of dibenzothiophene to phenanthrene and pristane to phytane as indicators of depositional environment and lithology of petroleum source rocks," *Org. Geochem.* **17**, 3581–3598 (1995).
- G. A. James and J. G. Wynd, "Stratigraphic nomenclature of Iranian oil consortium agreement area," *AAPG Bull.* **49** (12), 2182–2245 (1995).
- S. Z. Jassim and H. C. Goff, "Geology of Iraq". (Dolin, Prague and Moravian Museum, Brno, 2006).
- J. M. Moldowan, W. K. Seifert, and E. J. Gallegos, "Relationship between petroleum composition and depositional environment". *AAPG Bull.* **69**, 1255–1268 (1985).
- H. Motiei, *An Introduction to Zagros Petroleum Reservoirs Evaluation, (For Geologists)*, 1st ed. Vol. 2 (2010) [In Persian].
- A. P. Murray, R. E. Summons, C. J. Boreham, and L. M. Dowling, "Biomarker and alkane isotope profiles for Tertiary oils: relationship to source rock depositional setting". *Org. Geochem.* **22**, 521–542 (1994).
- M. Kobraei, Ph.D. Thesis (Tehran PolyTechnic University, Amir Kabir, 2016).
- M. Kobraei, J. Sadouni, and A. R. Rabbani, "Organic geochemical characteristics of Jurassic petroleum system in Abadan Plain and north Dezful zones of the Zagros basin, southwest Iran", *J. Earth Syst. Sci.* **128**:50 (2019). <https://doi.org/10.1007/s12040-019-1082-0>
- M. Kobraei, A. R. Rabbani, and F. Taati, "Lower Cretaceous Source rock Investigation in Western Zagros Basin—Southwest Iran," *J. Petrol. Explor. Prod. Technol.* (2017). <https://doi.org/10.1007/s13202-017-0362-y>
- K. E. Peters, and M. R. Cassa, "Applied source rock geochemistry," *The Petroleum System—From Source to Trap*, Ed. by L. B. Magoon and W. G. Dow, *AAPG Mem.* **60**, 93–120 (1994).
- K. E. Peters, C. C. Walters, and J. M. Moldowan, "The Biomarker Guide. Biomarkers and Isotopes in Petroleum Exploration and Earth History", (University of Cambridge Press, Cambridge, 2005), vol. 2, pp. 475–1155.
- J. K. Pitman, D. Steinshouer, M. D. Lewan, "Petroleum generation and migration in the Mesopotamian Basin and Zagros Fold Belt of Iraq: results from a basin—modeling study". *GeoArabia* **9** (4), 41–72 (2004).
- M. Radke, P. Garrigues, and H. Willsch, "Methylated dicyclic and tricyclic aromatic hydrocarbons in crude oils from the Handil field, Indonesia". *Org. Geochem.* **15**, 17–34 (1990).
- M. Radke, D. H. Welte, and H. Willsch, "Geochemical study on a well in the western Canada basin; relation of the aromatic distribution pattern to maturity of organic matter," *Geochim. Cosmochim. Acta* **46**, 1–10 (1982).
- M. Radke, "Application of aromatic compounds as maturity indicators in source rocks and crude oils". *Mar. Petrol. Geol.* **5**, 224–236, (1985).
- Y. Satarzadeh, J. W. Cosgrove, C. Vita Finzi, "The interplay of faulting and folding during the evolution of the Zagros deformation belt," *Forced Folds and Fractures*, Ed. by J. W. Cosgrove and M. S. Ameen, *Geol. Soc. Spec. Publ. London* **169**, 187–196 (2000).
- P. R. Sharland, M. Archer, D. M. Casey, et al. "Arabian Plate Sequence Stratigraphy". *GeoArabia Spec. Publ.*, No. 2, (2001).
- Z. Sofer, "Stable carbon isotope composition of crude oils; application to source depositional environment and petroleum alteration". *AAPG Bull.* **68**, 31–49 (1984).
- J. Stocklin, "Possible ancient continental margins in Iran," *The Geology of Continental Margins*, Ed. by C. A. Burk, & C. L. Drake (Springer, New York, 1974), pp. 873–887.
- E. A. Subroto, R. Alexander, R. I. Kagi, "30-Norhopanes: their occurrence in sediments and crude oils," *Chem Geol.* **93**, p. 179–192, (1991).
- G. H. Taylor, M. Teichmüller, A. Davis, C. F. K. Diessel, R. Littke, and P. Robert, *Organic Petrology* (Gebrüder-Borntraeger, Berlin—Stuttgart, 1998).
- B. P. Tissot, and D. H. Welte, *Petroleum Formation and Occurrence*, 2nd Ed. (Springer, New York, 1984).
- J. K. Volkmann, R. Alexander, R. I. Kagi, R. A. Noble, and G. W. Woodhouse, "A geochemical reconstruction of oil generation in Barrow sub-basin of Western Australia," *Geochim. Cosmochim. Acta* **47**, 2091–2106 (1983).
- H. M. Weiss, A. Wilhelms, N. Mills, J. Scotchmer, P. B. Hall, K. Lind, and T. Brekke, NIGOGA – "The Norwegian Industry Guide to Organic Geochemical Analyses [online]." Edition 4.0 Norsk Hydro, Statoil, Geolab Nor, SINTEF Petroleum Research and the Norwegian Petroleum Directorate. Available from World Wide Web: <<http://www.npd.no/engelsk/nigoga/default.htm>> (cited 24.08.11) (2000).
- A. Zeinalzadeh and A. Sajjadian, "Investigation of source rock zones in Darquain oilfield by petrophysical and Rock Eval data," *J. Sci. Tehran Univ.* **35**, 63–70 (2009) (In Persian).
- A. Zeinalzadeh, R. Moussavi-Harami, A. Mahboubi, and V. A. Sajjadian, "Basin and petroleum system modeling of the Cretaceous and Jurassic source rock of the gas and oil reservoirs in Darquain field, south west Iran," *J. Nat. Gas Sci. Eng.*, **26**, 419–426 (2015).
- D. Zhang, D. Huang, and L. Jinchao, "Biodegraded sequences of Karamay oils and semi quantitative estimation of their biodegraded degrees in Junggar Basin, China," *Org. Geochem.* **13**, 295–302 (1988).